

Glass-forming liquids and the glass transition: The energy landscape approach to dynamics and thermodynamics

SRIKANTH SASTRY

Jawaharlal Nehru Centre for Advanced Scientific Research, Jakkur Campus, Bangalore 560 064, India.

email: sastry@jncasr.ac.in

Received on November 18, 2004.

Abstract

Most liquids, under suitable conditions, are capable of transforming into glass, which is a microscopically disordered, solid form of matter. Glass formation occurs in the laboratory because the viscosity of the liquid becomes very high, causing the liquid to fall out of equilibrium on experimental time scales. Whether a true thermodynamic transition underlies the laboratory transformation is among the questions that remains to be answered. Another major theme of research activity is directed towards understanding the microscopic mechanisms leading to the dramatic growth of viscosity of liquids at low temperatures. Significant progress has recently been made by focusing attention on quantitative aspects of the energy landscape of glass-forming liquids. An outline of the approach is presented here, along with applications of the approach to studying thermodynamic and dynamic phenomena that take place when a liquid is cooled towards the glass transition, including: (i) The onset of *slow dynamics*; (ii) The crossover in dynamics to a regime of ‘activated dynamics’; (iii) The relationship between fragility (which quantifies the rapidity of change of dynamics as the glass transition is approached) and quantifiable features of the energy landscape; and (iv) The relationship between the ultimate boundaries of the liquid state, the liquid–gas spinodal (at which liquid becomes thermodynamically unstable) and the glass transition line (at which liquid transforms into an amorphous solid).

Keywords: Glass-forming liquids, glass transition, thermodynamics, dynamics, energy landscape.

1. Introduction

A wide variety of materials can exist at low temperatures in the form of a glass, which is *amorphous*, i.e. a form of matter lacking in any long-range structural order, but possessing mechanical properties of a solid [1–7]. For many materials, the glass state is a *metastable state*, and the state of the material in equilibrium is a crystalline solid. For some, notably polymers [8], the equilibrium crystalline structure, if it exists, is never attained and the glass is, for practical purposes, *the* state of the material at low temperatures. Examples of glasses are abundant both in nature and among man-made materials. Most of the water in the universe is expected to be in the glassy form, in cometary tails [9]. A part of the earth’s crust, in the form of amorphous silica formed during volcanic activity, is in the glassy state [10]. Window glass, whose dominant component is silica, is a man-made variant of the same material. A significant fraction of industrial plastics are glasses. Even among the metals, which are almost exclusively crystalline solids, metallic glasses have been of interest of late for their unusual and desirable material properties [11].

While amorphous solids can be prepared in many ways (e.g. depositing vapour on a cold substrate, or by application of pressure to a crystalline solid), the *conventional* method of preparing a glass is to cool a liquid in a fashion that prevents crystallisation (in cases where the crystal forms the equilibrium state at low temperatures). Correspondingly, the term ‘glass transition’ is used to designate the transformation of a liquid upon cooling to low temperatures into an amorphous solid. As described later, many interesting phenomena develop as a liquid is cooled towards the glass-transition temperature, which bear directly on the glass state. While understanding glasses as materials, with specific properties, require analysis of the synthesis, the chemical and physical properties of these amorphous solids at temperatures below the glass transition, general understanding of the nature of the glass state is also to be sought by studying materials in the liquid state, close to the glass transition. The work outlined in this article falls in the category of studies which approach the glass transition from the ‘liquid state’; the object of study is the glass-forming liquid at low temperatures, approaching the glass transition temperature from above.

The next three sections of this article describe briefly some salient aspects of the phenomenology of the glass transition, Section 3 the approach to analysing dynamic and thermodynamic aspects of glass formation by studying the properties of local potential energy minima sampled by the liquid, and Section 4 computer simulation methods employed in performing these analyses. Theoretical approaches to studying the glass transition, other than the energy landscape approach, are not specifically dealt, although reference is made to some, where appropriate. The subsequent sections describe the results of investigations on specific aspects of the phenomenology of liquids approaching the glass transition. The final section describes some related questions not discussed in detail, as well as future directions of investigation.

2. Phenomenology of glass formation

A brief overview of the phenomenology of glass formation is described in this section. Further details may be found in various recent reviews on the subject [1–7]. The purpose here is simply to introduce some aspects that will be referred to later on.

The dynamical and transport behaviour of a liquid may be characterised in various ways, such as by studying the diffusion of individual atoms or molecules, the manner in which fluctuations in local density decay (which allows estimation of a *relaxation time*), measuring rotational diffusion and relaxation if one considers molecular liquids, and measuring the viscosity. Viscosity, microscopic relaxation times and diffusivity in liquids are closely related. Similarly, the equilibrium, thermodynamic state is characterised by measuring quantities such as the heat capacity and bulk density.

A prerequisite for glass formation is that crystallisation is averted, which is typically achieved by cooling the liquid faster than a rate that may be estimated based on the temperature variation of viscosity and rates of nucleation of the crystal. For many glass formers, viscosity displays a strong temperature dependence, which deviates substantially from the Arrhenius temperature dependence, $\eta = \eta_0 \exp(E/k_B T)$ which is used to describe the temperature dependence of many dynamical quantities in a variety of systems. The most familiar ‘glass’, silica, however exhibits close to Arrhenius temperature dependence. A ge-

neric functional form that appears more suitable is the Vogel–Fulcher–Tammann–Hesse (VFT) form,

$$\eta = \eta_0 \exp\left(\frac{A}{T - T_0}\right). \quad (1)$$

Such a form predicts the viscosity to become arbitrarily large, and diverge at a finite temperature T_0 . However, when the viscosity reaches a value of around 10^{13} poise (which roughly corresponds to relaxation times of hundreds of seconds), liquids no longer achieve equilibrium under standard experimental conditions and time scales. Such falling out of equilibrium is also manifested in pronounced (but not discontinuous) changes in the temperature dependence of thermodynamic quantities such as the heat capacity and bulk density. Since the heat capacity of a liquid is generally higher than that of the corresponding crystal, the entropy of the liquid decrease with temperature faster than that of the crystal. Consequently, the *excess* entropy of the liquid (relative to the crystal), by extrapolation, appears to vanish at a finite temperature, as pointed out by Kauzmann [12], and referred to as the Kauzmann paradox. Resolution of this paradox, among other possibilities, involves the existence of an *ideal* glass transition, where the entropy associated with the degeneracy of *configurations* a liquid can assume vanishes. However, the slow down of dynamics and the existence of a thermodynamic transition are in principle two independent issues, as emphasised by various authors (see, e.g., [13]).

A second aspect of *slow dynamics* that becomes manifest as the glass transition temperature is approached is the time evolution of various relaxation processes. A convenient, and commonly used, probe is the relaxation of density fluctuations, measured by, for example, the van Hove self correlation function

$$G_s(r, t) = \frac{1}{N} \sum_{i=1}^N \langle \delta(|\mathbf{r}_i(t) - r(0)| - r) \rangle, \quad (2)$$

which describes the probability of finding at time t a particle at distance r from its location at $t = 0$. The time evolution of the Fourier transform of $G_s(r, t)$, the self intermediate scattering function $F_s(k, t)$ is exponential decay at high temperatures, while at lower temperatures, the Kohlrausch–Williams–Watts stretched exponential form,

$$F_s(k, t) = f(k) \exp\left[-\left(\frac{t}{\tau(T)}\right)^{\beta(T)}\right] \quad (3)$$

provides a good fit to the long-time behaviour. Values of $\beta < 1$, which are obtained at low temperatures, imply that the relaxation cannot be viewed as being characterised by a single *exponential* process (or time scale), but is slower.

At temperatures close to the glass transition, a breakdown of the Stokes–Einstein relation between the diffusion coefficient D and the viscosity η is observed. The Stokes–Einstein relation predicts an inverse relationship, $D/k_B T \eta$, between D and η [6, 14–17]. The measured

diffusivities are considerably larger than the predictions based on measured viscosities. At the same time, rotational diffusion continues to be well correlated with viscosity, implying a decoupling of rotational and translational diffusion. These and related observations are currently seen as manifestations of *heterogeneous dynamics* [6, 18, 19]. The distribution of relaxation times becomes sufficiently wide that quantities (such as viscosity and diffusion coefficient) which involve different averages over these relaxation times will begin to display qualitative differences with respect to temperature regimes where the relaxation times are narrowly distributed [20–22]. In particular, the picture is that the dynamics becomes *spatially* heterogeneous at low temperatures. Aspects of such spatially heterogeneous dynamics have also been studied by computer simulations, although at considerably higher temperatures than in experiments [23, 24]. Among the observations of the simulation studies is the identification of a growing *dynamical* correlation length scale [25–27].

Another manifestation of the slow down of dynamics, which occurs both above and below the laboratory glass transition, is the phenomenon of *aging*—the glass-forming liquid or glass continues to *anneal* on experimental times scales, and consequently, static as well as dynamic properties of the system continue to change over long time scales. The time translational invariance seen in systems in equilibrium is not observed. While this feature has been studied in the past [28], there has been considerable recent activity aimed at understanding such out of equilibrium behaviour [29].

3. The energy landscape approach

The disordered structure of a liquid has the implication that the energies of interaction between particles will generally be very complicated, and that the part of configuration space explored by the material in the liquid state is characterised by the presence of many local minima of the potential energy. Such is the case also, for example, in a crystalline solid if one allows for the presence of defects. The use of the phrase ‘energy landscape’ to describe the complicated interactions in a glass-forming liquid (and other disordered systems) therefore contains in addition the expectation that the complicated potential energy topography plays an essential role in determining the properties of the system. If such is the case, it is desirable to attempt a description of glass-forming liquids in terms of quantities that define the nature of the potential energy landscape. In the inherent structure approach [30], one considers the decomposition of the $3N$ dimensional (for an atomic liquid) configuration space of the liquid into basins of individual local potential energy minima, termed inherent structures (IS). A basin of a given minimum is defined as the set of points in the configuration space (or configurations) which map to that minimum under a local energy minimisation. The canonical partition function of the liquid can then be expressed as a sum over IS basins, the summand being partial partition functions defined for individual basins. In the following, the equations are written for a two-component atomic liquid, since the model liquids discussed in subsequent sections are such liquids. In turn, the sum over basins is written in terms of (a) a distribution of minima in energy, and (b) the free energies of basins, as follows:

$$Q(N, \rho, T) = \Lambda^{-3N} \frac{1}{N_A! N_B!} \int d\mathbf{r}^N \exp[-\beta \Phi] \quad (4)$$

$$\begin{aligned}
&= \sum_{\alpha} \exp[\beta \Phi_{\alpha}] \Lambda^{-3N} \int_{V_{\alpha}} d\mathbf{r}^N \exp(-\beta(\Phi - \Phi_{\alpha})) \\
&= \int d\Phi \Omega(\Phi) \exp[-\beta(\Phi + F_{vib}(\Phi, T))] \\
&= \int d\Phi \exp[-\beta(\Phi + F_{vib}(\Phi, T) - T S_c(\Phi))]
\end{aligned}$$

where Φ is the total potential energy of the system, α indexes individual IS, Φ_{α} is the potential energy at the minimum, $\Omega(\Phi)$ is the number density of IS with energy Φ , and the configurational entropy density $S_c \equiv k_B \ln \Omega$. The *basin free energy* $F_{vib}(\Phi_{\alpha}, T)$ is obtained by a restricted partition function sum over a given IS basin, V_{α} . Λ is the de Broglie wavelength, N_A and N_B are the number of *A* and *B* type atoms in the two-component liquid, T is the temperature, and ρ the density of the liquid. In the following, the dependence on ρ is not explicitly stated always since the interest is in T dependent behaviour at constant density. The configurational entropy of the liquid arises from the multiplicity of local potential energy minima sampled by the liquid at temperature T , and is related to the configurational entropy density above by

$$S_c(T) = \int d\Phi S_c(\Phi) P(\Phi, T), \quad (5)$$

where

$$\begin{aligned}
P(\Phi, T) &= \Omega(\Phi) \exp[-\beta(\Phi + F_{vib}(\Phi, T))] / Q(N, \rho, T), \\
&= \exp[-\beta(\Phi + F_{vib}(\Phi, T) - T S_c(\Phi))] / Q(N, \rho, T),
\end{aligned} \quad (6)$$

is the probability density that IS of energy Φ are sampled at temperature T . In the above expression for the partition function, an assumption has been made that the basin free energy does not differ for different basins of the same IS energy. Without reference to the distribution of minima, the configurational entropy can be defined as the difference of the total entropy of the liquid and the vibrational entropy of typical minima sampled at a given temperature:

$$S_c(\rho, T) = S_{total}(\rho, T) - S_{vib}(\rho, T). \quad (7)$$

The ‘entropy theory’ of Gibbs coworkers [31, 32] defines the ideal glass transition, underlying the laboratory transition, as an ‘entropy vanishing’ transition where the configurational entropy vanishes (the configurational entropy is not, however, defined in precisely the same way in [31, 32]). A similar picture also emerges from the study of mean field spin glass models and calculations motivated by them [33–35]. Whether such a transition exists for real materials is still a matter of debate [36, 37]. The calculations below produce such an entropy vanishing transition but it must be kept in mind that they result from extrapolations which may not be valid.

Further, Adam and Gibbs theory [32] relates the configurational entropy to relaxation times in the liquid:

$$\tau = \tau_0 \exp\left[\frac{A}{TS_c}\right]. \quad (8)$$

where A_0 is a material specific constant. The validity of this relation has been verified by numerous experimental studies (which typically use the *excess* entropy of the liquid over the crystal in place of S_c) and computer simulation studies [38–41] (where configurational entropy is evaluated). Further, if S_c has the form $TS_c = K_{AG}(T/T_K - 1)$, the Adam–Gibbs relation results in the VFT form (1), which may be written as

$$\tau = \tau_0 \exp\left[\frac{1}{K_{VFT}(T/T_0 - 1)}\right], \quad (9)$$

where T_0 is the temperature of apparent divergence of viscosity. K_{VFT} is a material specific parameter quantifying the *kinetic* fragility. Fragility is a measure of how rapidly the viscosity, relaxation times, etc. of a liquid changes as the glassy state is approached [42]. Small values of K_{VFT} yield temperature dependence close to the Arrhenius form, while large values yield super-Arrhenius behaviour.

That the basin-free energy F_{vib} arises from ‘vibrational’ motion within individual basins is emphasised by the suffix *vib*. If this motion is sufficiently localised around the minima, a suitable procedure would be to approximate the basins as harmonic wells, and to evaluate the basin-free energy within this approximation. The validity of such a procedure has been tested recently in various studies [34, 40, 41, 43–45]. It is found that below the temperature where the liquid begins to exhibit aspects of *slow dynamics* (non-Arrhenius behaviour of relaxation times, and stretched exponential relaxation)[43, 45, 46], a harmonic approximation of the basins is reasonable. However, this is not to be expected generally [39, 47], nor is it a requirement for calculating basin entropies. With a suitable criterion for defining inherent structure basins, one may also use constrained ensemble methods to evaluate the basin entropy [48, 49]. One must also consider whether results for classical systems typically studied in theoretical and computational studies hold for real systems.

In the harmonic approximation, the basin free energy is given simply in terms of the $3N$ vibrational frequencies that may be evaluated by diagonalizing the matrix of second derivatives, at a given local energy minimum, of the potential energy:

$$F_{vib} = k_B T \sum_{i=1}^{3N} \ln \frac{h\nu_i}{k_B T}, \quad (10)$$

or equivalently, the basin entropy,

$$\frac{S_{vib}}{k_B} = \sum_{i=1}^{3N} 1 - \log\left(\frac{h\nu_i}{k_B T}\right), \quad (11)$$

where ν_i are the vibrational frequencies of the given basin, and h is Plank’s constant. From the form of S_{vib} it is apparent that the entropy difference between two basins arises solely due to the difference in their frequencies. Thus, such entropy differences remain finite as

$T \rightarrow 0$ which is unphysical as the basin entropy of each basin and therefore their difference must go to zero for $T = 0$. An estimation of the effect of a quantum mechanical, as opposed to classical, treatment indicates that the effect of this artefact is not severe, if one considers deviations of the classical result at the glass transition temperature [50].

Calculations based on eqn. (11), where the vibrational frequencies are obtained numerically for energy minima generated in simulations, indicate [41] (see also [47, 51]) that the difference in S_{vib} , between basins is roughly linear in the basin energy. Thus one can write

$$\Delta S_{vib}(\Phi) \equiv S_{vib}(\Phi, T) - S_{vib}(\Phi_0, T) = \delta S(\Phi - \Phi_0), \quad (12)$$

and correspondingly,

$$F_{vib}(\Phi, T) = F_{vib}(\Phi_0, T) - T \delta S(\Phi - \Phi_0), \quad (13)$$

where Φ_0 is a reference basin energy. The latter expression follows since the internal energy $U_{vib} = 3Nk_B T$ for all basins.

In addition to the basin free energy, the partition function in eqn (4) requires knowledge of the configurational entropy density S_c . Various recent studies have explored methods for estimating S_c from computer simulations [41, 43, 44, 49, 52, 53]. It has been observed that the distribution $\Omega(\Phi)$ is well described by a Gaussian [41, 52, 54] (equivalently, $S_c(\Phi)$ an inverted parabola). The arguments [52, 54] may not apply to low energy minima, nor are expected to be valid for all systems; indeed, a recent computational study of a model of silica [55] reveals a nonGaussian $\Omega(\Phi)$, but this is related to a transition in silica from fragile to strong behaviour. Nevertheless, a Gaussian form for $\Omega(\Phi)$ allows for a straightforward evaluation of the partition function eqn (4), and whose validity has been tested in the range of temperatures where simulations are performed [41, 45].

The configurational entropy density is written as

$$\frac{S_c(\Phi)}{Nk_B} = \alpha - \frac{(\Phi - \Phi_0)^2}{\sigma^2} \quad (14)$$

where α is the height of the parabola and determines the total number of configurational states, i.e. energy minima (the total number is proportional to $\exp(\alpha N)$), Φ_0 and σ^2 , respectively, define the mean and the variance of the distribution. The parameters α , Φ_0 and σ have been estimated from simulation data [41]. With the above form for $S_c(\Phi)$ and eqn (13) for the vibrational free energy, the partition function can be evaluated, from which the following temperature dependence of the configurational entropy, the ideal glass transition temperature T_K (defined by $S_c(T_K) = 0$ and the IS energies are obtained:

$$\langle \Phi \rangle(T) = \Phi_0^{\text{eff}} - \frac{\sigma^2}{2Nk_B T}, \quad (15)$$

where $\Phi_0^{\text{eff}} = \Phi_0 \frac{\sigma^2 \delta S}{2Nk_B}$,

$$TS_c(T) = K_{AG}^{PEL}(T)(T/T_K - 1); \quad K_{AG}^{PEL}(T) = \left(\frac{\sigma \sqrt{\alpha}}{2} + \frac{\sigma^2 \delta S}{4Nk_B} \right) \left(1 + \frac{T_K}{T} \right) - \frac{\sigma^2 \delta S}{2Nk_B}, \quad (16)$$

and

$$T_k = \sigma(2Nk_B\sqrt{\alpha} + \sigma\delta S)^{-1}. \quad (17)$$

These equations constitute relations that express quantities relevant to the thermodynamics of glass-forming liquids, the configurational entropy and the ideal glass transition temperature, in terms of parameters that describe the ‘energy landscape’ of the liquid, namely the distribution of local energy minima, and the topography of individual minima in the form of vibrational frequencies. In particular, the expressions for TS_c shows that the fragility of the liquid can be expressed in terms of parameters that quantify the ‘energy landscape’ of the liquid. In particular, they show that when variations in basin entropy (with the energy of the minima) are unimportant, the spread in energy of the distribution of minima determines the fragility. When such variation is significant, it contributes to the fragility; if basin entropies (at the same temperature) are bigger for higher energy minima (which is the situation expected in the experimental, constant pressure conditions), there results a decrease in the fragility, as well as a decrease in the ideal glass transition temperature. The results here show that the use of excess entropy as a surrogate for the configurational entropy can be misleading. In view of the broad experimental test of the Adam–Gibbs relation, it has been suggested recently [56] that excess entropy and configurational entropy may vary proportionally. If one defines the excess entropy, not with respect to the crystal as is normally done, but with respect to the ‘ideal glass’ (i.e., the lowest energy minimum), then one obtains an expression for the excess entropy as

$$TS_{ex}(T) = K_{ex}^{PEL}(T)(T/T_K - 1), \quad (18)$$

where K_{ex} is the fragility index based on the excess entropy, given by,

$$K_{ex}^{PEL}(T) = \left(\frac{\sigma\sqrt{\alpha}}{2} + \frac{\sigma^2\delta S}{4Nk_B} \right) \left(1 + \frac{T_K}{T} \right). \quad (19)$$

Comparison of the expressions for K_{ex}^{PEL} and $K_{ex}^{PEL}(T)$ show that indeed they are closely related, but there is no proportionality in a strict sense. However, there are in principle subtle issues (e.g. in the analysis above T_K is used as a scaling temperature, but the existence of a Kauzmann temperature is itself an open question) that remain to be sorted out in how fragility is measured.

4. Computer simulations

The results presented in the subsequent sections are obtained from computer simulations of two model atomic liquids. Since the study of dynamics is an objective, with some exceptions so noted, the molecular dynamics (MD) simulations are used to generate equilibrium trajectories of a few hundred particles, employing conventional methods (see e.g. [57]). Since the dynamics slows down considerably at the lowest temperatures studied, run lengths of up to 0.4 μ s (in Argon units) are used. From such trajectories, a sample of configurations is used to perform local energy minimizations (using the conjugate gradient method[58]) to obtain inherent structures. In evaluating basin free energies, the matrix of

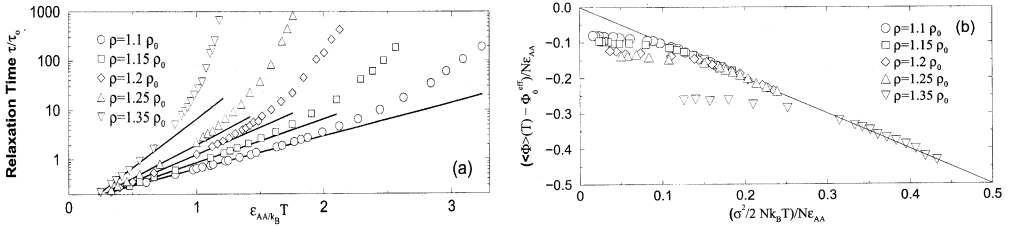


FIG. 1. (a) Relaxation times for a range of densities for the ‘80:20’ binary mixture shown in an Arrhenius plot, indicating deviation from Arrhenius behaviour at low temperatures. (b) Scaled plot of inherent structure energies showing a $1/T$ temperature dependence at low temperatures, and deviations away from $1/T$ dependence at high temperatures. The crossover between these two regimes corresponds to the onset of non-Arrhenius T -dependence of relaxation times. At low temperatures, the behaviour confirms the prediction in eqn (15). Adapted from [45].

second derivatives of the potential energy (Hessian) is diagonalized for the inherent structures, to obtain normal mode frequencies. All the simulations are done at constant density.

Except when noted (Sec.s) the results are for a (‘80:20’) binary mixture of 204 type A and 52 type B particles, interacting via the Lennard–Jones (LJ) potential, with parameters $\epsilon_{AB}/\epsilon_{AA} = 1.5$, $\epsilon_{BB}/\epsilon_{AA} = 0.5$, $\sigma_{AB}/\sigma_{AA} = 0.8$, and $\sigma_{BB}/\sigma_{AA} = 0.88$, and $m_B/m_A = 1$. This system has been extensively studied as a model glass former [59]. A quadratic cutoff [60] is imposed on the potential at distance $2.5\sigma_{\alpha\beta}$. The second (‘50:50’) model liquid contains 251 particles of type A and 249 particles of type B interacting via a binary Lennard–Jones potential with parameters $\sigma_{BB}/\sigma_{AA} = 5/6$, $\sigma_{AB} = (\sigma_{AA} + \sigma_{BB})/2$, and $\epsilon_{AA} = \epsilon_{AB} = \epsilon_{BB}$. The masses are given by $m_B/m_A = 1/2$. The length of the sample is $L = 7.28 \sigma_{AA}$ and the potential was cut and shifted at $2.5\sigma_{\alpha\beta}$. All quantities are reported in reduced units: T in units of ϵ_{AA}/k_B , lengths in units of σ_{AA} , densities in units of $\rho_0 = \sigma_{AA}^{-3}$ and time in units of $\tau_0 \equiv (\sigma_{AA}^2 m / \epsilon_{AA})^{1/2}$ in the first case, and $\tau_0 \equiv (m_B \sigma_{AA}^2 / 48\epsilon)^{1/2}$ in the second. Argon units for the A type particles are used to represent some of the data. Further details about the simulations can be found in [40, 41, 46, 61].

5. Onset of slow dynamics

As noted earlier, the onset of super-Arrhenius temperature dependence of viscosity, diffusivity, etc. and non-exponential decay of correlations are characteristic features of glass-forming liquids. While the problem of slow dynamics had been discussed by many in ‘energy landscape’ terms, the general expectation was that its influence on liquid properties arose at temperatures close to the glass transition. However, it was shown in [46] that signatures of the influence of the liquid’s energy landscape manifest in the same temperature range where one observes the onset of slow dynamics.

Figure 1(a) shows, in an Arrhenius plot ($\log \tau$ vs $1/T$), the relaxation times τ obtained from the self intermediate scattering function $F_s(k, t)$ introduced earlier, for the ‘80:20’ binary mixture, for a range of densities. At each density, one may identify a ‘crossover’ or onset temperature T_s across which the T dependence of τ become non-Arrhenius. It was observed in [46] that this onset temperature also marks a change in the manner the system explores the energy landscape. At higher T , the average potential energy of the IS is nearly

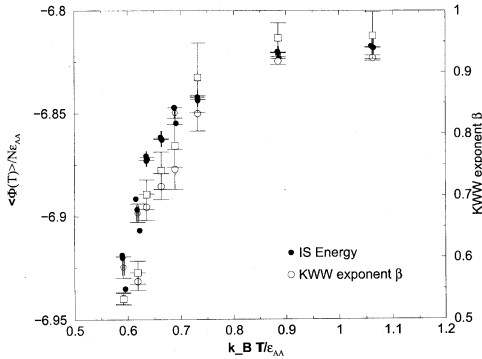


FIG. 2. The temperature dependence of the inherent structure (IS) energy and the KWW exponent β for the ‘50:50’ binary mixture. Deviations in β away from 1 closely track the deviations of the IS energy from the high temperature plateau. Adapted from [62]. Four independent samples for the energy, and two different estimations for β . (from the MD trajectory, and from ‘inherent dynamics’; see Section 6). Adapted from [62].

constant, while at lower T one sees considerable temperature dependence. In other words, the system begins to explore deeper energy minima below T_s . A more quantitative analysis was done in [45] where it is shown that below the onset temperature, the $1/T$ temperature dependence for the average IS energy (described in the previous section) holds, while it breaks down at higher temperatures. This is shown in Fig. 1(b) where the scaling form predicted in eqn (15) is used. Since the prediction is based on a harmonic approximation to the IS basins, this data may be seen as evidence that the nature of the energy landscape sampled by the liquid (and hence the basin structure) undergoes a change at T_s for which further evidence is shown in [45].

Figure 2 shows, for the ‘50:50’ binary mixture [62], the temperature dependence of the average IS energy, along with that of the KWW stretch exponent β (obtained from fits to self intermediate scattering function $F_s(k, t)$), which shows a remarkable coincidence in the manner of their deviations from the corresponding high temperature values. Very similar results are also obtained in the case of water [47, 63].

Relatively little attention has been paid to the temperature range of the onset of slow dynamics, with both theoretical and experimental work focused more on phenomena at lower temperatures. One approach that places emphasis on the onset regime is frustrated domain theory [64]. There have, however, been many recent studies [53, 65–68] where an onset temperature (or density) is discussed, which may be identified with the onset temperature discussed above, or which have explicitly been discussed in reference to the analysis in [45, 46].

6. Crossover to activated dynamics

An early discussion of the importance of considering the role of potential energy barriers was by Goldstein [69] who proposed that there exists a crossover temperature T_x , where the shear relaxation time is $\sim 10^{-9}$ s, below which relaxation is governed by thermally activated crossings of potential energy barriers. Subsequently, T_x has been identified [70] with the dynamical transition temperature described by mode coupling theory [71]. Till recently, however, no direct test of this correspondence was available. Recent work has to a substantial degree clarified the meaning of this correspondence.

In [46], the structure of the basins of inherent structures obtained at temperatures straddling the mode coupling temperature [59] were probed by generating trajectories starting

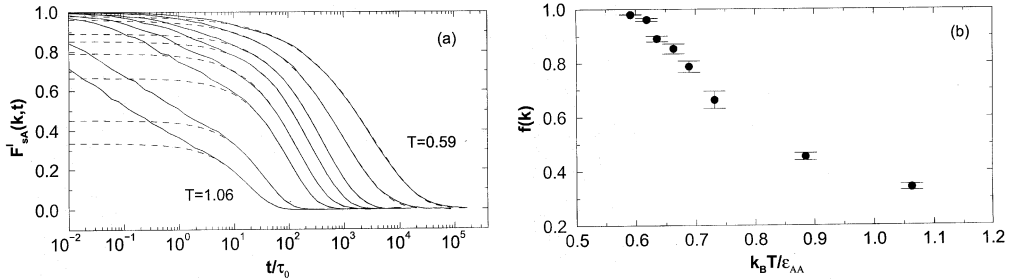


FIG. 3. (a) The self intermediate scattering function of A particles, from the time series of inherent structures, along with fits to the KWW stretched exponential form in eqn (3). (b) Coefficients $f(k)$ from the KWW fits above vs temperature. Adapted from [61].

from these structures, at very low temperatures (far below the glass transition temperature). While for the lower T inherent structures, the distribution of displacements away from them is close to Gaussian, supporting the expectation that the basin structure is harmonic, for high T , distributions with multiple peaks are obtained, spanning much larger distances, indicating that the inherent structures at the higher T are separated by negligible energy barriers, and that the system can easily escape to neighbouring basins with very little excitation energy. This observation is both consistent with Goldstein's observations, as well as simulation results at temperatures above the mode coupling temperature for water [72, 73].

A more direct analysis was performed in [61], where the MD trajectories of the '50:50' binary mixture, for a range of temperatures, was mapped to the corresponding time series of inherent structures. For basins separated by significant energy barriers, it is reasonable to have a picture of the dynamics as a series of intra-basin 'vibrations' interrupted by periodic transitions between basins. If the two processes are clearly separated, the dynamics revealed by the time series of IS should contain no contribution from intra-basin vibrations. Therefore, unlike the correlation functions from the MD trajectory which reveal both a short time decorrelation interpreted to be due to 'vibrational' motion (or 'cage-rattling'), as well as long time structural relaxation, correlation functions obtained from the time series of inherent structure should reveal only the long time relaxation. Figure 3(a) shows the self intermediate scattering function $F_s(k, t)$ obtained from the IS time series, from which it is seen that (a) at high temperatures, the IS dynamics still retains a substantial component of relaxation that is not part of the long-time relaxation, and (b) as temperature is lowered, such contribution due to short time relaxation decreases, and appears to disappear at the lowest studied temperature. This trend can be quantified by the coefficient $f(k)$ in eqn (3), which is shown in Fig. 3(b). It is seen that $f(k)$ approaches 1 as $T \rightarrow T_c$ (T_c is estimated from relaxation times [61]), thereby providing a clear characterisation of the crossover described by Goldstein, and associated with the mode coupling transition temperature T_c . Recently, for the Kob–Andersen binary Lennard–Jones system, it has been found that the diffusivities of the liquid display a crossover to Arrhenius behaviour around and below the mode coupling temperature [74], much like the crossover seen in silica [55]. The significance of this observation needs to be evaluated by further studies, including finite size analysis.

A further development along these lines has been the investigation recently of the properties of saddle points to which typical configurations of a liquid map, as a function of tem-

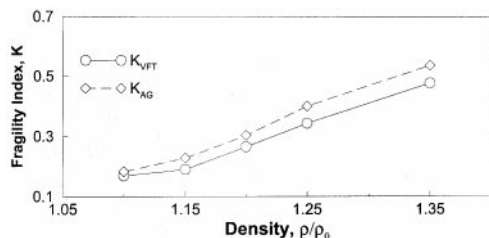


FIG. 4. Kinetic and thermodynamic fragilities calculated (a) from VFT fits to diffusivities, and (b) from the expression for the configurational entropy in eqn (16). Adapted from [41].

perature [75, 76]. These studies show that the order of the saddles (i.e. the number of negative curvature directions) approaches zero at the mode coupling temperature, so that at low temperatures, the typical configurations of the liquid are close to minima rather than to saddles. These analyses also make contact with the instantaneous normal mode approach [77, 78], which will be discussed further later.

7. Thermodynamic analysis of fragility

Fragilities are typically calculated and compared for substances which display many differences among them, which complicates a discussion of specific differences between them that might be responsible for their different fragilities. A simple way, used here, to vary fragility while keeping other properties the same, is to vary the density of the same liquid. For the '80:20' binary mixture, the kinetic fragilities (eqn (9)) are obtained by calculating the diffusivities for a number of temperatures at fixed density, at five different densities (Fig. 4). The approach taken to perform a thermodynamic analysis of fragility is to (test the validity of and) use the Adam–Gibbs relation. The methods used for calculating the configurational entropy are outlined in Section 6 and in [40, 41]. Figure 5 shows the (logarithm of) diffusivities plotted against $(TS_c)^{-1}$. The Adam–Gibbs relation predicts that the diffusivities in such a plot would fall on a straight line, which is indeed seen to be the case at each density. The slopes of the individual curves do not coincide, and this represents a limitation of the extent to which the Adam–Gibbs relation is predictive. This point will be discussed later. Results in Fig. 4 imply that it is reasonable to seek a connection between dynamical properties of a liquid and thermodynamic properties through the Adam–Gibbs relation. The thermodynamic fragility obtained from the average slope of TS_c vs T/T_K in the range where diffusivities are measured, is shown in Fig. 4. The thermodynamic fragilities agree with the kinetic fragilities (obtained from diffusivities) to quite a reasonable degree. Figure 6 shows the configurational entropy densities (log of the distribution Ω of minima) estimated in the process of calculating the configurational entropy, which shows that with increasing density of the liquid (a) the total number of energy minima present (quantified by α ; see eqn (14)) decreases, and (b) the width σ and the span of the distribution ($2\sigma\alpha^{1/2}$) increase. From eqn (16), the span of the distribution is seen to be a key factor controlling the fragility of the liquid, which is borne out by the data in Fig. 6. In the case of the liquid studied, the contribution from the variation of basin entropies is not substantial. However, previous analyses of experimental data indicate that basin entropies can vary substantially and have been incorporated in calculations [79–83]. Analysis of such cases where basin entropy changes play a significant role is desirable to substantiate results presented here.

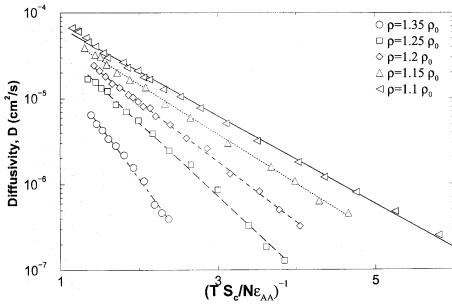


FIG. 5. The Adam–Gibbs plot of diffusivities against configurational entropy. At each density, the data are well represented by straight lines, consistently with the Adam–Gibbs prediction. Adapted from [41].

8. The glass transition and the liquid–gas spinodal

The glass transition represented an ultimate boundary to the liquid state, in the sense that while the liquid–crystal phase boundary may be ‘trespassed’ by the liquid remaining in a metastable state upon supercooling, such a retention of the liquid state is not possible below the glass transition temperature. Another such ultimate boundary is the liquid–gas spinodal, which is reached when a liquid is superheated or subjected to negative pressure. It is of interest to understand the relationship between these two limits to the liquid state; the motivation for the analysis presented here comes from observations made in [84] where a threshold density was identified for a monoatomic model liquid across which the structure of typical IS sampled by the liquid undergoes a qualitative change, from compact structures at higher densities to spatially heterogeneous, ‘fissured’ structures (exhibiting system spanning voids) at lower densities. It is also observed that the pressure calculated for the IS displays a minimum at the threshold density identified geometrically [85]. Two speculations made in [84] arising from these observations were: (i) the threshold density closely approximates the $T \rightarrow 0$ limit of the liquid–gas spinodal, and (ii) the same density also forms the lower density limit to glass formation. In the simplest scenario, the two loci (the glass transition curve in the temperature–density plane, and the liquid–gas spinodal line) representing ultimate boundaries to the liquid state approach $T = 0$ at the threshold density, and thus exhibit a complementarity in the range of densities in which they are operative. These ideas were tested in [40] for the ‘80:20’ binary mixture. The threshold density is located from the minimum of the pressure vs density curve. The liquid–gas spinodal curve is estimated from (a) restricted ensemble Monte Carlo (REMC) simulations, (b) calculating the isothermal compressibility K_T from constant temperature and volume simulations and ex-

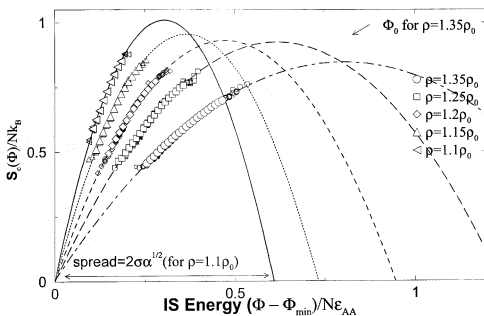


FIG. 6. The distribution of minima estimated from simulation data following the method described in Section 7, represented by the configurational entropy density (see eqn (5)). The larger data points are averages of estimates from individual temperatures (shown in smaller symbols). The continuous lines are Gaussian fits (eqn (14)). Adapted from [41].

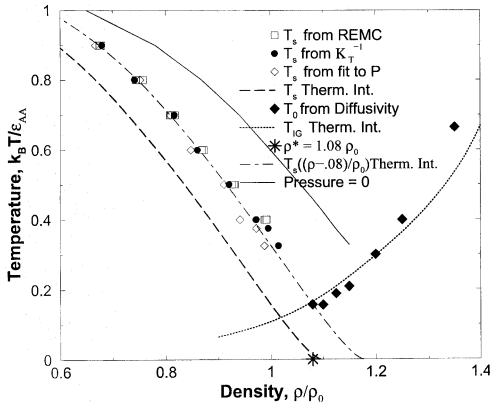


FIG. 7. Liquid–gas spinodal obtained from (a) REMC simulations, (b) k_T , (c) polynomial fits to isotherms, and (d) the empirical free energy (T_s Therm. Int.’). The same curve is also shown shifted in ρ by 0.08 ($T_s(\rho - 0.08)$ Therm. Int.’). The glass transition locus obtained from (e) VFT fits to diffusivity data, and (d) extrapolation of configurational entropy to zero (T_{IG} Therm. Int.’). Also marked (*) is the density ρ^* where inherent structure pressure is a minimum. The zero pressure curve is also shown for reference. Adapted from [40].

trapolating $k_T^{-1} \rightarrow 0$, (c) obtaining polynomial fits to isotherms and locating the minima of the curve at each temperature, and (d) from calculating the equation of state from an empirical free energy function based on equilibrium simulation data (labelled ‘Therm. Int.’ in the figure). The details of these methods are described in [40]). The glass transition locus is obtained from (i) VFT fits to diffusivity data (thus a kinetic estimate) and from estimating the thermodynamic, ideal glass transition locus from the empirical free energy. The results are shown in Fig. 7, which demonstrate that the two curves intersect at a finite temperature, contrary the speculation in [84]. However, the density at which they intersect is indeed the threshold density. The simple scenario (where the two curves intersect at $T = 0$) has been obtained in a recent calculation [86], but it appears at present that such a scenario might be a special case. Whether the threshold density has a clearly definable significance in the general case remains to be studied. An interesting outcome of the scenario shown in Fig. 7 is the prediction that a locus of ideal glass–gas mechanical instability must exist. Such a possibility is strongly supported, for example, by experimental data [87] on liquids which show a negatively sloped (in the pressure temperature plane) line of glass transitions, implying an intersection with the liquid–gas spinodal at finite temperatures.

9. Related questions and future directions

The results described above illustrate the utility of focusing attention of aspects of the energy landscape explored by the liquid in elucidating the nature of the slow down of dynamics in liquids at low temperature and the glass transition. While the ability to calculate configurational entropy and test the Adam–Gibbs relation in recent studies has been very useful, as Fig. 5 illustrates, it also highlights the limitations of configurational entropy by itself to predict dynamical properties. In this regard, recent work [75–78] focusing on properties of saddle points, and in particular, exploration of relationship between configurational entropy of liquids to such more detailed descriptions [77, 78] is likely to be very fruitful. Since the generally accepted derivation of the Adam–Gibbs relation exists, work on these lines will serve to rationalise a widely employed notion. One of the important questions *not* addressed in this article is the existence of an ideal glass transition. Based on an analysis of inherent structure statistics, Stillinger [37] has presented an argument against the existence of a Kauzmann temperature. While the existence of an ideal glass transition is not relevant

to understanding the slow dynamics in liquids *per se*, it is nevertheless an important question in its own right. This argument, which relies on considerations concerning local defects that may occur in amorphous inherent structures, has recently been tested numerically by generating inherent structures for a model liquid. The results concerning defects in inherent structures conform to Stillinger's description [88]. A counter to Stillinger's argument is that inherent structures are not necessarily 'suitable objects' to discuss the possible existence of a thermodynamic transition. For example, notwithstanding an analogy that can be made, inherent structures are not equivalent to metastable states in mean-field spin models which display a 'Kauzmann' temperature. The characterisation of the appropriate analog for systems with finite range interactions, and its relation to inherent structures, are open questions [89, 90]. On the other hand, in the case of realistic systems, some of the results discussed here indicate that the inherent structure approach affords one the ability to address fairly detailed questions (e.g. the fragile-to-strong crossover in silica [55] recently studied, or the analysis of fragility presented here) and a means to refine relevant concepts. Regarding the analysis of fragility, it is desirable to further establish the link between parameters quantifying the energy landscape and fragility, and more importantly, to develop an understanding of how these parameters may be tuned in real systems. Further study of the relationship between the liquid-gas spinodal and the glass transition curve, and possible experimental verification of the glass-gas mechanical instability, constitute another direction for future work.

References

1. Review articles in *Science* **267** (1995).
2. P. G. Debenedetti, *Metastable liquids*, Princeton University Press (1996).
3. M. D. Ediger, C. A. Angell, and S. R. Nagel, Supercooled liquids and glasses, *J. Phys. Chem.*, **100**, 13200–13212 (1996).
4. C. A. Angell, K. L. Ngai, G. B. McKenna, P. F. McMillan, and S. W. Martin, Relaxation in glassforming liquids and amorphous solids, *J. Appl. Phys.*, **88**, 3113–3157 (2000).
5. *Proc. of Unifying Concepts in Glass Physics*, Trieste, 1999, *J. Phys. Cond. Mat.*, **12** (2000).
6. M. D. Ediger, Spatially heterogeneous dynamics in supercooled liquids, *A. Rev. Phys. Chem.*, **51**, 99–128 (2000).
7. P. G. Debenedetti, and F. H. Stillinger, Supercooled liquids and the glass transition, *Nature*, **410**, 259–267 (2001).
8. E. A. DiMarzio, Equilibrium-theory of glasses, *Ann. N.Y. Acad. Sci.*, **371**, 1–20 (1981).
9. P. Jenniskens, and D. F. Blake, Structural transitions in amorphous water ice and astrophysical implications, *Science*, **265**, 753–756 (1994).
10. M. K. Bose, *Igneous petrology*, World Press, Calcutta (1997).
11. A. L. Greer, Metallic glasses, *Science*, **267**, 1947–1953 (1995).
12. W. Kauzmann, The nature of the glassy state and the behavior of liquids at low temperatures, *Chem. Rev.*, **43**, 219–256 (1948).
13. J. Kurchan, Recent theories of glasses as out of equilibrium systems, *C. R. Acad. Sci. Paris, t.2, Serie IV*, 2001, 239–247; <http://arXiv.org/abs/cond-mat/0011110>
14. F. Fujara, B. Geil, H. Sillescu, and G. Fleischer, Translational and rotational diffusion in supercooled orthoterphenyl close to the glass-transition, *Z. Phys. B*, **88**, 195–204 (1992).
15. I. Chang, F. Fujara, B. Geil, G. Heuberger, and H. Sillescu, Translational and rotational molecular motion in supercooled liquids studied by NMR and forced Rayleigh scattering, *J. Non-Cryst. Solids*, **172–174**, 248–255 (1994).

16. M. T. Cicerone, F. R. Blackburn, and M. D. Ediger, How do molecules move near T_g ? Six probes in o-terphenyl across 14 decades in time, *J. Chem. Phys.*, **102**, 471–479 (1995).
17. G. Heuberger, and H. Sillescu, Size dependence of tracer diffusion in supercooled liquids, *J. Phys. Chem.*, **100**, 15255–15260 (1996).
18. E. V. Russel, and N. E. Israeloff, Direct observation of molecular cooperativity near the glass transition, *Nature*, **408**, 695–698 (2000).
19. E. R. Weeks, J. L. Crocker, A. C. Levitt, A. Schofield, and D. A. Weitz, Three-dimensional direct imaging of structural relaxation near the colloidal glass transition, *Science*, **287**, 627–629 (2000).
20. G. Tarjus and D. Kivelson, Breakdown of the Stokes–Einstein relation in supercooled liquids, *J. Chem. Phys.*, **103**, 3071–3073 (1995).
21. F. H. Stillinger, and J. A. Hodgdon, Translation-rotation paradox for diffusion in fragile glass-forming liquids, *Phys. Rev. E*, 1994, **50**, 2064–2068 (1994).
22. S. Bhattacharya, and B. Bagchi, Decoupling of tracer diffusion from viscosity in a supercooled liquid near the glass transition, *J. Chem. Phys.*, **107**, 5852–5862 (1997).
23. M. M. Hurley, and P. Harrowell, Kinetic structure of a two-dimensional liquid, *Phys. Rev. E*, **52**, 1694–1698 (1995).
24. C. Donati, J. F. Douglas, W. Kob, S. J. Plimpton, P. H. Poole, and S. C. Glotzer, Stringlike cooperative motion in a supercooled liquid, *Phys. Rev. Lett.*, **80**, 2338–2341 (1998).
25. C. Dasgupta, A. V. Indrani, S. Ramaswamy, and M. K. Phani, Is there a growing correlation length near the glass transition?, *Europhys. Lett.*, **15**, 307–312 (1991).
26. C. Bennemann, C. Donati, J. Baschnagel, and S. C. Glotzer, Growing range of correlated motion in a polymer melt on cooling towards the glass transition, *Nature*, **399** 246–249 (1999).
27. S. Franz, and G. Parisi, On non-linear susceptibility in supercooled liquids, *J. Phys. Cond. Mat.*, **12**, 6335–6342 (2000).
28. L. C. Struick, *Physical aging in amorphous polymers and other materials*, Elsevier (1978).
29. J.-P. Bouchaud, L. F. Cugliandolo, J. Kurchan, and M. Mezard, Out of equilibrium dynamics in spinglasses and other glassy systems, in *Spin glasses and random fields*, A. P. Young (ed.), World Scientific (1998).
30. F. H. Stillinger, and T. A. Weber, Hidden structure in liquids, *Phys. Rev. A*, **25**, 978–989 (1982); Packing structures and transitions in liquids and solids, *Science*, **228**, 983–989 (1984); F. H. Stillinger, A topographic view of supercooled liquids and glass formation, *Science*, **267**, 1935–1939 (1995).
31. J. H. Gibbs, and E. A. Di Marzio, Nature of the glass transition and the glassy state, *J. Chem. Phys.*, **28**, 373–383 (1958).
32. G. Adam, and J. H. Gibbs, On the temperature dependence of cooperative relaxation properties in glass-forming liquids, *J. Chem. Phys.*, **43**, 139–146 (1965).
33. T. R. Kirkpatrick, and D. Thirumalai, p-spin-interaction spin–glass models: Connections with the structural glass problem, *Phys. Rev. B*, **36**, 5388–5397 (1987); T. R. Kirkpatrick and P. G. Wolynes, Stable and metastable states in mean-field Potts and structural glasses, *Phys. Rev. B*, **36**, 8552–8564 (1987); T. R. Kirkpatrick, D. Thirumalai, and P. G. Wolynes, Scaling concepts for the dynamics of viscous liquids near an ideal glassy state, *Phys. Rev. A*, **40**, 1045–1054 (1989).
34. B. Coluzzi, G. Parisi, and P. Verrocchio, Lennard–Jones binary mixture: A thermodynamical approach to glass transition, *J. Chem. Phys.*, **112**, 2933–2944 (2000); B. Coluzzi, G. Parisi, and P. Verrocchio, Thermodynamical liquid–glass transition in a Lennard–Jones binary mixture, *Phys. Rev. Lett.*, **84**, 306–309 (2000); B. Coluzzi, M. Mezard, G. Parisi, and P. Verrocchio, Thermodynamics of binary mixture glasses, *J. Chem. Phys.*, **111**, 9039–9052 (1999); M. Mezard, and G. Parisi, Thermodynamics of glasses: A first principles computation, *Phys. Rev. Lett.*, **82**, 747–750 (1999).
35. M. Cardenas, S. Franz, and G. Parisi, Glass transition and effective potential in the hypernetted chain approximation, *J. Phys. A: Math. Gen.*, **31**, L163–L169 (1998).

36. P. D. Gujrati, On the absence of the completely ordered phase in the Flory model of semi-flexible linear polymers, *J. Phys. A*, 1980, **13**, L437–L442; P. D. Gujrati, Lower bounds on entropy for polymer-chains on a square and a cubic lattice, *J. Stat. Phys.*, **28**, 441–472 (1982); P. D. Gujrati, and M. Goldstein, On the validity of the Flory–Huggins approximation for semiflexible chains, *J. Chem. Phys.*, **74**, 2596–2603 (1981).
37. F. H. Stillinger, Supercooled liquids, glass transitions, and the Kauzmann paradox, *J. Chem. Phys.*, **88**, 7818–7825 (1988).
38. R. J. Speedy, The hard sphere glass transition, *Mol. Phys.*, **95**, 169–178 (1998).
39. A. Scala, F. W. Starr, E. La Nave, F. Sciortino, and H. E. Stanley, Configurational entropy and diffusivity of supercooled water, *Nature*, **406**, 166–169 (2000).
40. S. Sastry, Liquid limits: Glass transition and liquid–gas spinodal boundaries of metastable liquids, *Phys. Rev. Lett.*, **85**, 590–593 (2000).
41. S. Sastry, The relationship between fragility, configurational entropy and the potential energy landscape of glass forming liquids, *Nature*, **409**, 164–167 (2001).
42. C. A. Angell, Relaxation in liquids, polymers and plastic crystals – Strong/fragile patterns and problems, *J. Non-Cryst. Solids*, **131–133**, 13–31 (1991).
43. F. Sciortino, W. Kob, and P. Tartaglia, Inherent structure entropy of supercooled liquids, *Phys. Rev. Lett.*, **83**, 3214–3217 (1999).
44. S. Buechner, and A. Heuer, The potential energy landscape of a model glass former: thermodynamics, anharmonicity, and finite size effects, *Phys. Rev. E*, **60**, 6507–6518 (1999); Metastable states as a key to the dynamics of supercooled liquids, *Phys. Rev. Lett.*, **84**, 2168–2171 (2000).
45. S. Sastry, Onset temperature of slow dynamics in glass forming liquids, *PhysChemComm.*, **3**, 79–83 (2000); (<http://arXiv.org/abs/cond-mat/0012054>).
46. S. Sastry, P. G. Debenedetti, and F. H. Stillinger, Signatures of distinct dynamical regimes in the energy landscape of a glass forming liquid, *Nature*, **393**, 554–557 (1998).
47. F. W. Starr, S. Sastry, E. La Nave, A. Scala, H. E. Stanley, and F. Sciortino, Thermodynamic and structural aspects of the potential energy surface of simulated water, *Phys. Rev. E*, **63**, 041201-1-041201-10 (2001).
48. R. J. Speedy, Constrained simulations to count the glasses that a fluid samples, *J. Molec. Struct.*, **485–486**, 537–543 (1999).
49. S. Sastry, Evaluation of configurational entropy of a model liquid from computer simulations, *J. Phys. Cond. Mat.*, **12**, 6515–6523 (2000).
50. S. Sastry, Inherent structure approach to the study of glass forming liquids, *Proc. Slow Dynamics and Freezing in Condensed Matter Systems*, J. Nehru University, New Delhi, 2000, *Phase Transitions*, **75**, 507–517 (2002); (<http://arXiv.org/abs/cond-mat/0101079>).
51. F. Sciortino, and P. Tartaglia, Extension of the fluctuation-dissipation theorem to the physical aging of a model glass-forming liquid, *Phys. Rev. Lett.*, **86**, 107–110 (2001).
52. R. J. Speedy, and P. G. Debenedetti, The distribution of tetravalent network glasses, *Mol. Phys.*, **88**, 1293–1316 (1996).
53. A. Crisanti, and F. Ritort, Potential energy landscape of finite-size mean-field models for glasses, *Europhys. Lett.*, **51**, 147–153 (2000).
54. A. Heuer, and S. Buechner, Why is the density of inherent structures of a Lennard–Jones-type system Gaussian?, *J. Phys. Cond. Mat.*, **12**, 6535–6543 (2000).
55. I. Saika-Voivod, P. H. Poole, and F. Sciortino, Fragile-to-strong transition and polyamorphism in the energy landscape of silica, *Nature*, **412**, 514–517 (2001).
56. L.-M. Martinez, and C. A. Angell, A thermodynamic connection to the fragility of glassforming liquids, *Nature*, **410**, 663–667 (2001).
57. M. P. Allen, and D. J. Tildesley, *Computer simulations of liquids*, Clarendon Press (1987).
58. W. H. Press, S. A. Teukolsky, W. T. Vetterling and B. P. Flannery, *Numerical recipes: The art of scientific computing*, 2nd edn, Cambridge University Press (1992).

59. W. Kob, and H. C. Andersen, Testing mode-coupling theory for a supercooled binary Lennard–Jones mixture: The van Hove correlation function, *Phys. Rev. E*, **51**, 4626–4641 (1995).
60. S. D. Stoddard, and J. Ford, Numerical experiments on the stochastic behavior of a Lennard–Jones gas system, *Phys. Rev. A*, **8**, 1504–1512 (1973).
61. T. B. Schröder, S. Sastry, J. C. Dyre, and S. C. Glotzer, Crossover to potential energy landscape dominated dynamics in a model glass-forming liquid, *J. Chem. Phys.*, **112**, 9834–9840 (2000).
62. S. Sastry, P. G. Debenedetti, F. H. Stillinger, T. B. Schröder, J. C. Dyre, and S. C. Glotzer, Potential energy landscape signatures of slow dynamics in glass forming liquids, *Physica A*, **270**, 301–308 (1999).
63. F. W. Starr, S. Sastry, F. Sciortino, and H. E. Stanley, Supercooled water: Dynamics, structure and thermodynamics, *Proc. DAE (India) Solid State Physics Symp.* 1999, R. Mukhopadhyay, B. K. Godwal and S. M. Yusuf (eds), Universities Press, 2000; *Solid St. Phys. (India)*, **42**, 77–80 (1999); (<http://arXiv.org/abs/cond-mat/0001296>).
64. S. A. Kivelson, D. Kivelson, X. Zhao, Z. Nussinov, and G. Tarjus, A thermodynamic theory of supercooled liquids as they get glassy, *Physica A*, **219**, 27–38 (1995); G. Tarjus, D. Kivelson and P. Viot, The viscous slowing down of supercooled liquids as a temperature-controlled super-Arrhenius activated process: a description in terms of frustration limited domains, *J. Phys. Cond. Mat.*, **12**, 6497–6508 (2000).
65. S. C. Glotzer, N. Jan, and P. H. Poole, The potential energy landscape of the \pm Ising spin glass, *J. Phys. Cond. Mat.*, **12**, 6675–6682 (2000).
66. C. Dasgupta, and O. T. Valls, Free energy landscape of simple liquids near the glass transition, *J. Phys. Cond. Mat.*, **12**, 6553–6562 (2000).
67. F. Affouard, and M. Descamps, Is there something of mode coupling theory in orientationally disordered crystals?, *Phys. Rev. Lett.*, **87**, 035501-1-035501-4 (2001).
68. S. Kamath, R. H. Colby, S. K. Kumar, and J. Baschnagel, Thermodynamic signature of the onset of caged dynamics in glass-forming liquids, *J. Chem. Phys.*, **116**, 865–868 (2002).
69. M. Goldstein, Viscous liquids and the glass transition: A potential energy barrier picture, *J. Chem. Phys.*, **51**, 3728–3739 (1969).
70. C. A. Angell, Perspective on the glass transition, *J. Phys. Chem. Sol.*, **49**, 863–870 (1988).
71. W. Götze, and L. Sjögren, Relaxation processes in supercooled liquids, *Rep. Prog. Phys.*, **55**, 241–376 (1992).
72. I. Ohmine, and H. Tanaka, Fluctuation, relaxations, and hydration in liquid water. Hydrogen-bond rearrangement dynamics, *Chem. Rev.*, **93**, 2545–2566 (1993).
73. F. Sciortino, and P. Tartaglia, Harmonic dynamics in supercooled liquids: The case of water, *Phys. Rev. Lett.*, **78**, 2385–2388 (1997).
74. S. S. Ashwin, and S. Sastry, Low temperature behaviour of the Kob–Andersen binary mixture, *J. Phys.: Condens. Matter*, **15**, S1253–S1258 (2003).
75. L. Angelani, R. Di Leonardo, G. Ruocco, A. Scala, and F. Sciortino, Saddles in the energy landscape probed by supercooled liquids, *Phys. Rev. Lett.*, **85**, 5356–5359 (2000).
76. K. Broderix, K. K. Bhattacharya, A. Cavagna, A. Zippelius, and I. Giardina, Energy landscape of a Lennard–Jones liquid: Statistics of stationary points, *Phys. Rev. Lett.*, **85**, 5360–5363 (2000).
77. T. Keyes, Entropy, dynamics, and instantaneous normal modes in a random energy model, *Phys. Rev. E*, **62**, 7905–7908 (2000).
78. E. La Nave, A. Scala, F. W. Starr, F. Sciortino, and H. E. Stanley, Instantaneous normal mode analysis of supercooled water, *Phys. Rev. Lett.*, **84**, 4605–4608 (2000).
79. M. Goldstein, Viscous liquids and the glass transition. V. Sources of the excess specific heat of the liquid, *J. Chem. Phys.*, **64**, 4767–4774 (1976).
80. C. A. Angell and K. J. Rao, Configurational excitations in condensed matter, and the bond lattice model for the liquid–glass transition, *J. Chem. Phys.*, **57**, 470–481 (1972).

81. J. L. Green, K. Ito, K. Xu, and C. A. Angell, Fragility in liquids and polymers: New, simple quantifications and interpretations, *J. Phys. Chem. B*, **103**, 3991–3996 (1999).
82. G. P. Johari, A resolution for the enigma of a liquid's configurational entropy-molecular kinetics relation, *J. Chem. Phys.*, **112**, 8958–8969 (2000).
83. G. P. Johari, Contributions to the entropy of a glass and liquid, and the dielectric relaxation time, *J. Chem. Phys.*, **112**, 7518–7523 (2000).
84. S. Sastry, P. G. Debenedetti, and F. H. Stillinger, Statistical geometry of particle packing. II. Weak spots in liquids, *Phys. Rev. E*, **56**, 5533–5543 (1997).
85. S. Sastry, D. S. Corti, P. G. Debenedetti, and F. H. Stillinger, Statistical geometry of particle packings. I. Algorithm for exact determination of connectivity, volume, and surface areas of void space in monodisperse and polydisperse sphere packings, *Phys. Rev. E*, **56**, 5524–5532 (1997).
86. P. G. Debenedetti, F. H. Stillinger, T. M. Truskett, and C. J. Roberts, The equation of state of an energy landscape, *J. Phys. Chem. B*, **103**, 7390–7397 (1999).
87. C. A. Angell, and Z. Qing, Glass in a stretched state formed by negative-pressure vitrification: Trapping in and relaxing out, *Phys. Rev. B, Rapid Commun.*, **39**, 8784–8787 (1989).
88. S. Sastry, Numerical test of Stillinger's argument concerning the Kauzmann paradox, *J. Phys. Chem. B*, **108**, 19698–19702 (2004).
89. G. Biroli and R. Monasson, From inherent structures to pure states: some simple remarks and examples, *Europhys. Lett.*, **50**, 155–161 (2000).
90. M. Mezard, First steps in glass theory, in *More is different: Fifty years of condensed physics* (N. P. Ong, and R. Bhatt, eds), p. 237, Princeton University Press (2002); (<http://arXiv.org/abs/cond-mat/0005173>).